Supporting Information

A Time Saving and Cost Effective Route for Metal Oxides Activation

Sajjad Ahmed Khan Leghari [a,c], *Shamaila Sajjad* [a,b]* *and Jinlong Zhang* [a]

[a] *Lab for Advanced Materials and Institute of Fine Chemicals, East China University of Science and Technology, 130 Meilong Road, Shanghai, 200237, P. R. China*

[b] *International Islamic University, H-10, Islamabad, Pakistan.*

[c] *Pakistan Institute of Engineering and Applied Sciences, Islamabad, Pakistan.*

E-mail: shalisajjad@hotmail.com

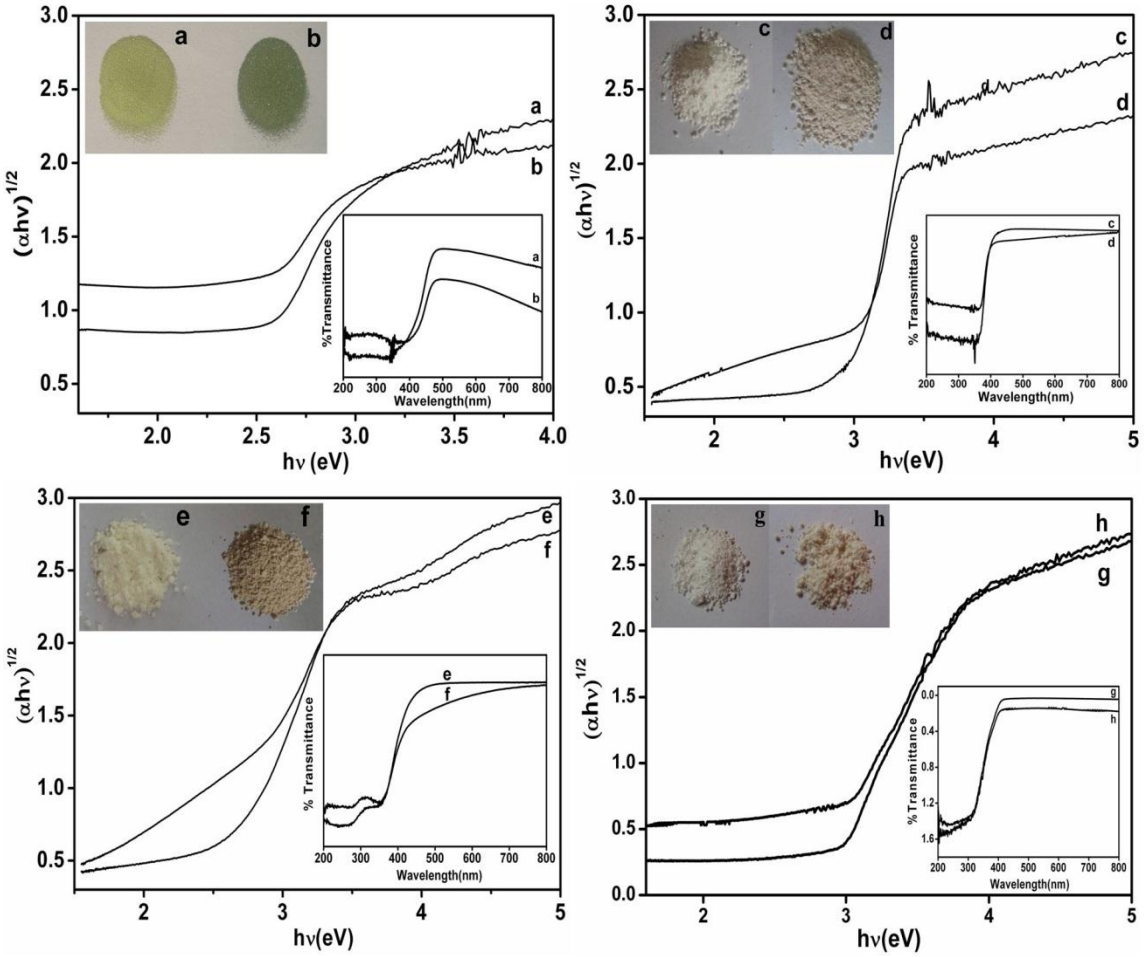

Figure S1. DRS plots of Kubelka-Munk function versus the energy of the light absorbed and photograph of different samples of metal oxides. (a) Pure WO_3; (b) Evacuated WO_3; (c) Pure ZnO; (d) Evacuated ZnO; (e) Pure CeO_2; (f) Evacuated CeO_2; (g) Pure Degussa P-25; (h) Evacuated Degussa P-25 and UV-Vis diffused transmittance spectra in the inset.

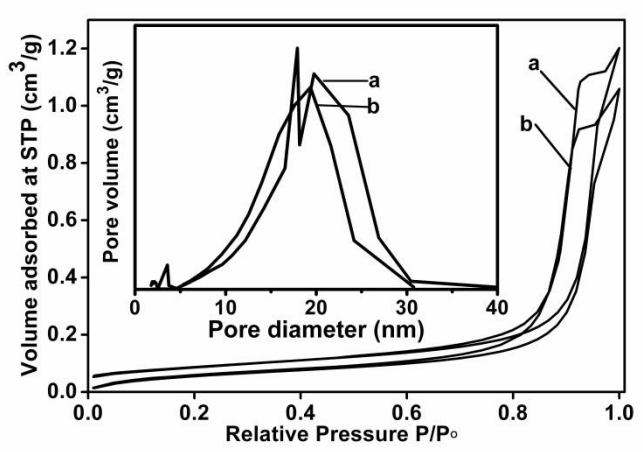

Figure S2. N_2 isotherms of different samples: (a) pure WO_3; (b) evacuated WO_3 and pore size distribution in the inset.

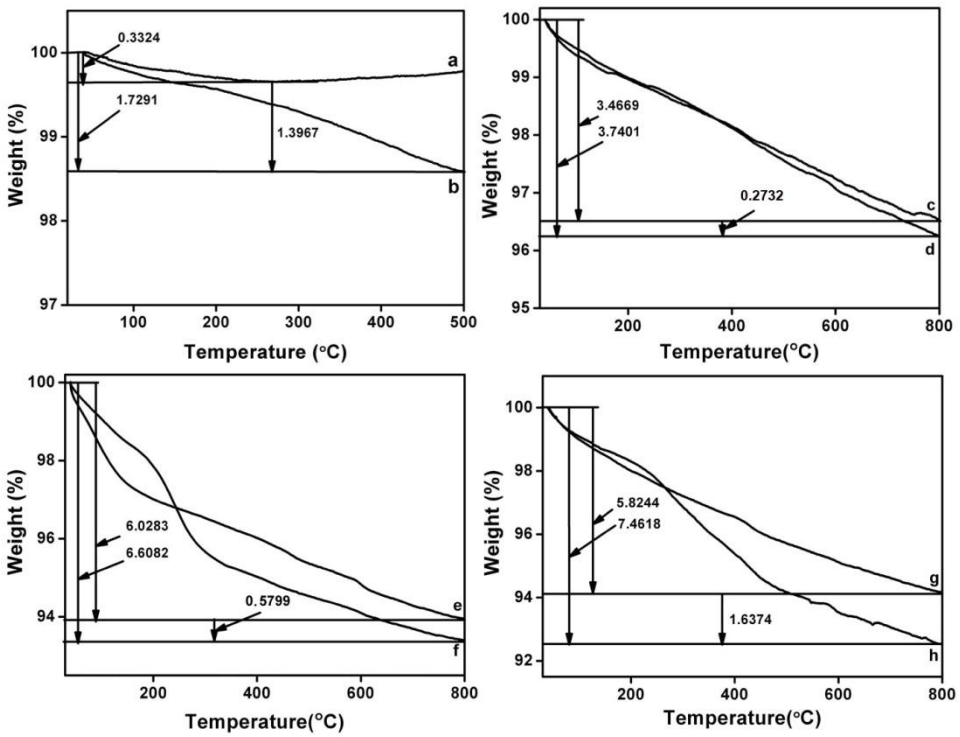

Figure S3. Thermo gravimetric analysis (TGA) of different samples (a) Pure WO_3; (b) Evacuated WO_3; (c) Pure ZnO; (d) Evacuated ZnO; (e) Pure CeO_2; (f) Evacuated CeO_2; (g) Pure Degussa P-25; (h) Evacuated Degussa P-25.

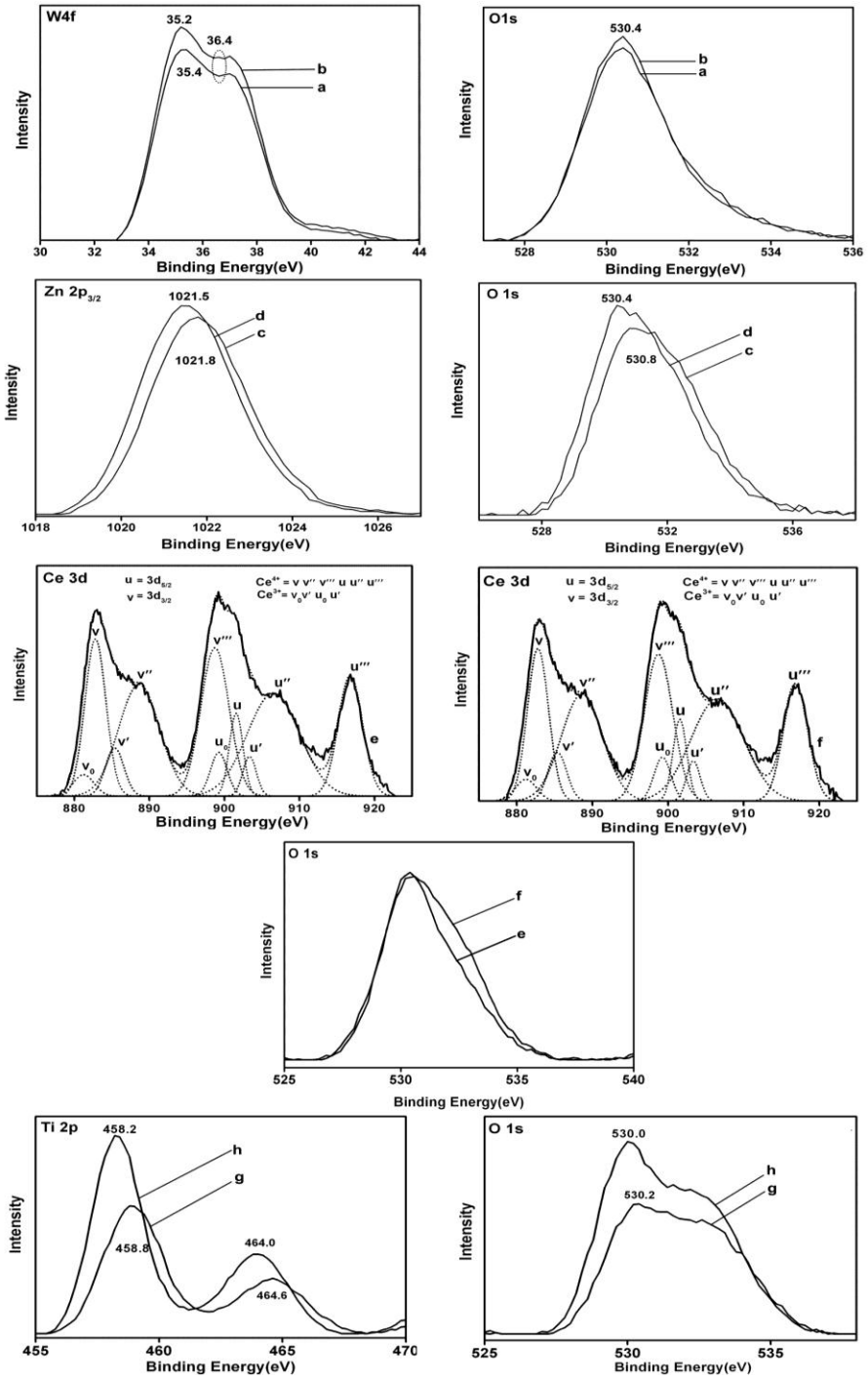

Figure S4. X-ray photoelectron spectra of different metal oxides: (a) Pure WO_3; (b) Evacuated WO_3; (c) Pure ZnO; (d) Evacuated ZnO; (e) Pure CeO_2; (f) Evacuated CeO_2; (g) Pure Degussa P-25; (h) Evacuated Degussa P-25.

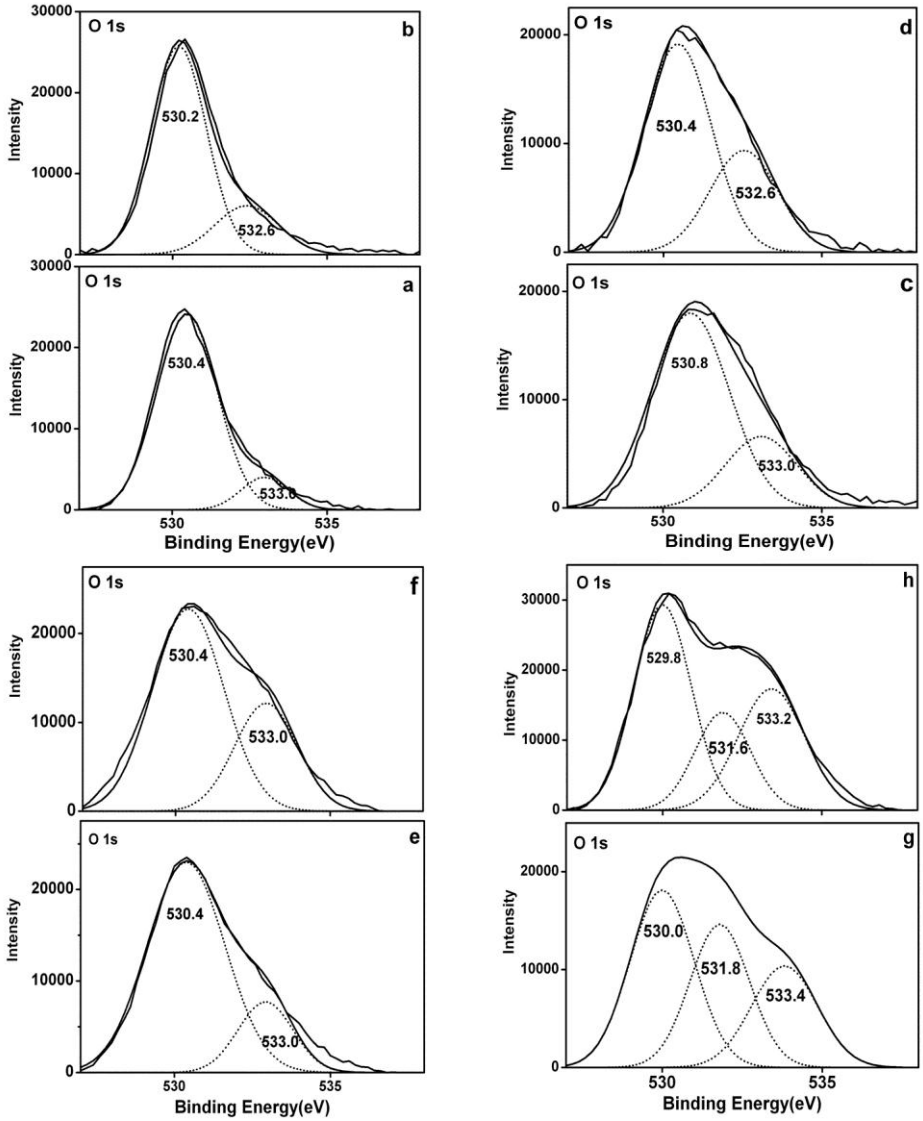

Figure S5. Deconvolution X-ray photoelectron spectra of O1s of different pure and evacuated metal oxides (a) Pure WO_3; (b) Evacuated WO_3: (c) Pure ZnO; (d) Evacuated ZnO; (e) Pure CeO_2; (f) Evacuated CeO_2; (g) Pure Degussa P-25 TiO_2 and (h) Evacuated Degussa P-25 TiO_2.

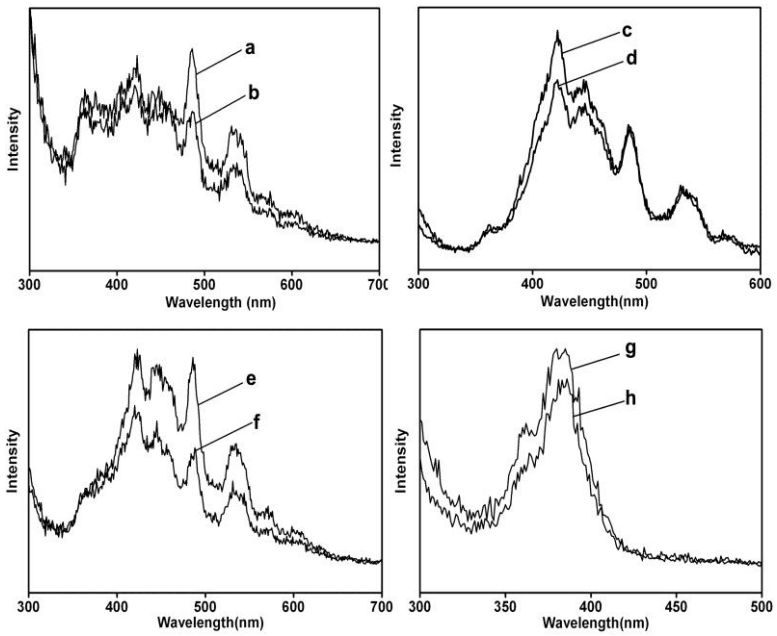

Figure S6. Photoluminescence spectra of different metal oxides: (a) Pure WO_3; (b) Evacuated WO_3; (c) Pure ZnO; (d) Evacuated ZnO; (e) Pure CeO_2; (f) Evacuated CeO_2; (g) Pure Degussa P-25 and (h) Evacuated Degussa P-25.

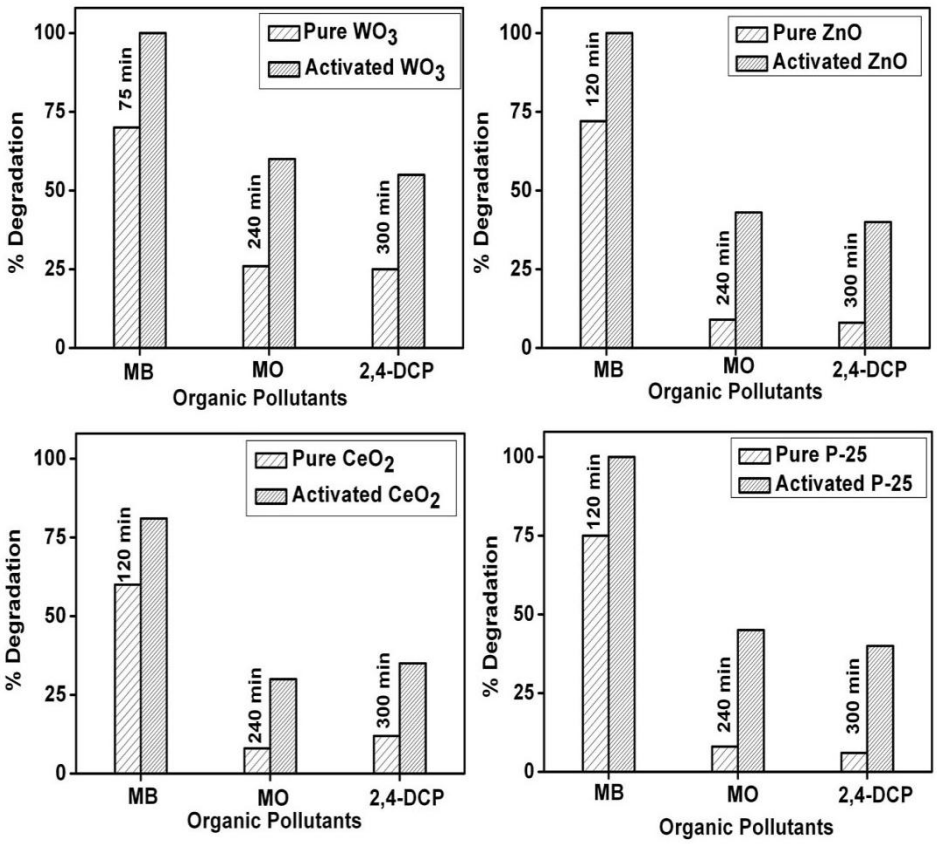

Figure S7. Comparative photo catalytic degradation profile of different pollutants over pure and evacuated metal oxides under visible light.

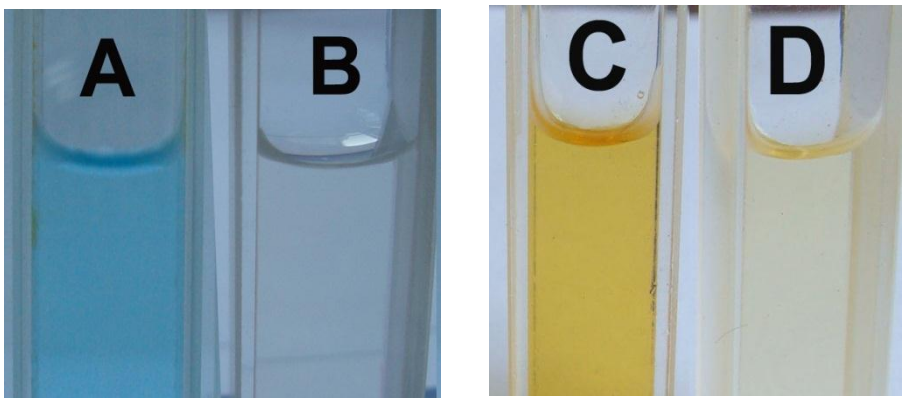

Figure S8. Photographs of photo degradation of 10 mgL^{-1} MB (A) before and (B) after visible light irradiation for 75 min. on the vacuum activated WO_3, and 10 mgL^{-1} MO (C) before and (D) after visible light (>420nm) irradiation for 6 hours on the vacuum activated WO_3.

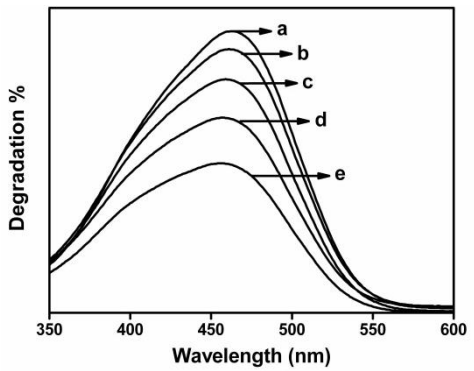

Figure S9. UV-Vis absorption spectra of MO in evacuated WO_3 suspensions after visible light (>420nm) irradiation for 3 hours (initial conc. of MO= 10mg L^{-1}, amount of catalyst = 1.0 g L^{-1}). a. pure absorption spectrum of MO dye b. adsorption of MO c. degradation after 1 h irradiation d. degradation after 2 h irradiation e. degradation after 3h.

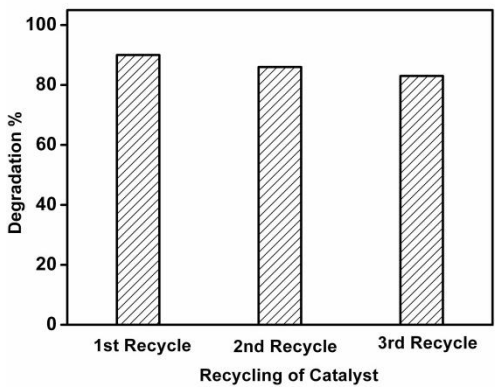

Figure S10. Recycling of catalyst for the photo degradation of 10 mgL^{-1} MO after visible light (>420nm) irradiation for 6 hours on evacuated WO_3.

Figure S11. Photo graphs of pure, vacuum activated WO_3 and evacuated WO_3 after the photo catalytic degradation reaction illustrating photo stability.

Table S1 Comparative X-ray diffraction parameters and BET surface area of different pure and evacuated metal oxides.

Samples	2θ	FWHM (2θ)	d-spacing [Å]	Crystallite size (nm)	BET area ($m^2 g^{-1}$)
WO_3- Comm.	23.399	0.286	3.6451	43.03 ± 3	6.88
WO_3- Evac.	24.480	0.329	3.6333	39.04 ± 3	5.01
ZnO- Comm.	36.240	0.503	2. 4767	20.05 ± 3	34.0
ZnO - Evac.	36.280	0.521	2. 4741	19.01 ± 3	27.0
CeO_2- Comm.	28.500	0.344	3.1293	9.63 ± 3	79.4
CeO_2- Evac.	28.520	0.329	3.1271	9.34 ± 3	67.2
P-25- Comm.	25.280	0.570	3. 5201	17.18 ± 3	51.4
P-25- Evac.	25.300	0.571	3.5174	17.14 ± 3	47.0